Synthesis and Characterization of the New Lead Strontium Germanate $PbSrGeO_4$

Lucas L. Petschnig[a], Klaus Wurst[a], Lukas Perfler[b], Dirk Johrendt[c], and Hubert Huppertz[a]

[a] Institut für Allgemeine, Anorganische und Theoretische Chemie, Leopold-Franzens-Universität Innsbruck, Innrain 80 – 82, A-6020 Innsbruck, Austria

[b] Institut für Mineralogie und Petrographie, Leopold-Franzens-Universität Innsbruck, Innrain 52f, A-6020 Innsbruck, Austria

[c] Department Chemie, Ludwig-Maximilians-Universität München, Butenandtstraße 5 – 13, D-81377 München, Germany

Reprint requests to H. Huppertz. E-mail: Hubert.Huppertz@uibk.ac.at

Z. Naturforsch. **2014**, *69b*, 845 – 850 / DOI: 10.5560/ZNB.2014-4125
Received June 13, 2014

The new lead strontium germanate $PbSrGeO_4$ was synthesized by a high-temperature solid-state reaction of lead(II) oxide, strontium carbonate, and germanium(IV) oxide at a temperature of 900 °C in a platinum crucible. The compound crystallizes in the orthorhombic space group $P2_12_12_1$ (no. 19) being isotypic to the structure of $BaNdGaO_4$ [1]. The primitive cell contains four formula units with lattice parameters of $a = 995.40(2)$, $b = 732.44(2)$, $c = 599.42(2)$ pm, $V = 437.02(2)$ Å^3, and residuals of $R_1 = 0.0385$ and $wR_2 = 0.0997$ for all data. The main structural element of $PbSrGeO_4$ is an isolated $[GeO_4]^{4-}$ tetrahedron. A circular arrangement of six of these $[GeO_4]^{4-}$ tetrahedra leads to the formation of large channels along *b* in which the strontium cations are eightfold coordinated by oxygen atoms. The lead cations are coordinated by three oxygen atoms, and with a lone pair of electrons they show a pseudo-tetrahedral coordination. Next to the structural investigations, $PbSrGeO_4$ was characterized by Raman-spectroscopic investigations and DFT calculations.

Key words: Germanate, Crystal Structure, Solid-state Reaction, DFT Calculations

Introduction

Borogermanates are known as new potential materials for nonlinear optical devices. In $Rb_2GeB_4O_9$ [2], $K_2GeB_4O_9 \cdot 2\,H_2O$ [3], and $(CH_3NH_3)_2GeB_4O_9$ [4], the efficiency in generating the second harmonic (SHG) is two times higher than in the well known reference material KDP. The designated aim of our research was to synthesize a new strontium borogermanate in the chemical system $SrCO_3$-GeO_2-H_3BO_3 *via* a high-temperature solid-state reaction and the use of a flux.

At the beginning of our project (July 2013), the group of alkaline earth metal borogermanates was represented by the compounds $Ca_{10}Ge_{16}B_6O_{51}$ [5], $Ba_3[Ge_2B_7O_{16}(OH)_2](OH)(H_2O)$ [6], and $Ba_3Ge_2B_6O_{16}$ [6]. A look into the literature revealed that there was a gap regarding strontium borogermanates. To obtain the missing strontium compound, we started with a typical solid state reaction of the reactands $SrCO_3$, GeO_2 and H_3BO_3. But in contrast to the procedure for the above mentioned calcium and barium borogermanates [5, 6], we additionally used a flux consisting of lead(II) and lead(IV) oxide. This kind of flux was already used in the high-pressure synthesis of the rare-earth borogermanate $Ce_6(BO_4)_2Ge_9O_{22}$ [7].

We obtained a golden-yellow product containing two different phases, none of them being a novel strontium borogermanate. Instead, we could identify in the powder X-ray diffraction pattern a well-known lead germanate with the chemical composition $Pb_5Ge_3O_{11}$ [8] and a new unknown phase. A single-crystal structure determination on crystals of the latter unknown phase revealed a new lead strontium germanate with the composition $PbSrGeO_4$ being isotypic to $BaNdGaO_4$ [1] and structurally related to the β-K_2SO_4 structure type [9, 10]. In this work, we report

about the synthesis, the single-crystal structure determination, DFT calculations, and Raman spectroscopic investigations of $PbSrGeO_4$.

Finally, it should be mentioned that our original goal of synthesizing the missing strontium borogermanate was achieved by the group of Mao *et al.*, who recently synthesized the first strontium borogermanates $SrGe_2B_2O_8$ and $Sr_3Ge_2B_6O_{16}$ [11]. Additionally, we were able to synthesize a third strontium borogermanate with the composition $Sr_{3-x/2}B_{2-x}Ge_{4+x}O_{14}$ ($x = 0.32$) [12].

Experimental Section

Synthesis

As mentioned above, the first synthesis took place in the system $SrCO_3$-GeO_2-H_3BO_3 in the presence of a flux consisting of PbO and PbO_2 in the ratio 24 : 0.6. This led to a heterogeneous product consisting of $Pb_5Ge_3O_{11}$ [8] and the new compound $PbSrGeO_4$. The fate and behavior of H_3BO_3 during this synthesis are not clear. Presumably it acts as a flux material which is amorphous in the final product mixture as it could not be detected in the powder diffractogram any longer.

As a consequence, in the next step, the stoichiometry of the reaction mixture was adapted to the composition $PbSrGeO_4$ according to Eq. (1) in order to see if $PbSrGeO_4$ can be obtained directly from the educts without H_3BO_3 and PbO_2 as flux materials.

$$PbO + SrCO_3 + GeO_2 \xrightarrow{900\,^\circ C} PbSrGeO_4 + CO_2 \quad (1)$$

The reaction mixture containing 102.6 mg $SrCO_3$ (99+ %, Merck, Darmstadt, Germany), 72.8 mg GeO_2 (99.99 %, ChemPur, Karlsruhe, Germany) and 155.2 mg PbO (99.7 %, Acros, Geel, Belgium) was ground together in an agate mortar and filled into a FKS 95/5 crucible (Feinkornstabilisiert, 95 % Pt, 5 % Au, Ögussa, Wien, Austria). The sample was heated up to 900 °C (Nabertherm muffle furnace) with a rate of 3 °C min^{-1} and held at that temperature for 130 h. After that period, the furnace was switched off and the reaction product naturally cooled down to room temperature. The new compound $PbSrGeO_4$ was obtained in the form of colorless, air- and water-resistant crystals. The powder diffraction pattern (Fig. 1) clearly exhibited $PbSrGeO_4$ as the major phase. Two tiny reflections marked with asterisks in the powder pattern could not be assigned up to now.

Crystal structure analysis

The powder diffraction pattern of $PbSrGeO_4$ was obtained in transmission geometry from a flat sample of the reaction product, using a Stoe Stadi P powder diffractometer with Ge (111)-monochromatized MoK_{α_1} ($\lambda = 70.93$ pm) radiation. The comparison of the experimental powder pattern with the theoretical pattern simulated from the single-crystal data in Fig. 1 has shown that they match well.

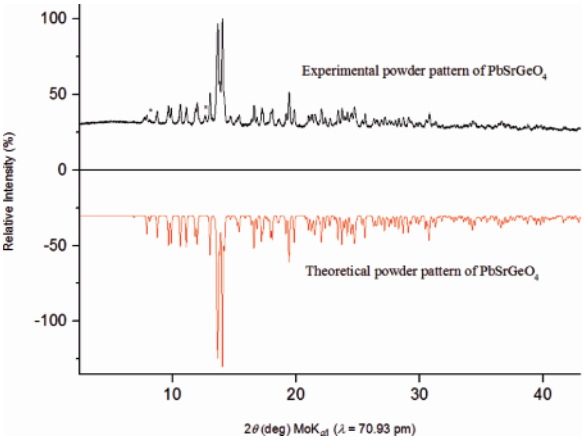

Fig. 1 (color online). Experimental powder pattern (top) of $PbSrGeO_4$ compared with the theoretical powder pattern (bottom) simulated from the single-crystal data.

Small single crystals of $PbSrGeO_4$ were isolated by mechanical fragmentation. The single crystal intensity data were collected at room temperature using a Nonius Kappa-CCD diffractometer with graphite-monochromatized MoK_α radiation ($\lambda = 71.073$ pm). A semiempirical absorption correction based on equivalent and redundant intensities (SCALEPACK [13]) was applied to the intensity data. All relevant details of the data collection and evaluation are listed in Table 1. From the systematic extinctions, the orthorhombic space group $P2_12_12_1$ was derived. The structure refinement was performed by taking the positional parameters of the isotypic phase $BaNdGaO_4$ [1] as starting values (SHELXL-13 [14, 15]). All atoms were refined with anisotropic displacement parameters, and the final difference Fourier synthesis did not reveal any significant residual peaks. The refinement exhibited that the measured crystal was a racemic twin, where the twin domains showed a ratio of 1 : 1. Positional parameters, anisotropic displacement parameters and interatomic distances are listed in the Tables 2 – 5. The program DIAMOND was used for the graphical representation of the structure [16].

Further details of the crystal structure investigation may be obtained from Fachinformationszentrum Karlsruhe, 76344 Eggenstein-Leopoldshafen, Germany (fax: +49-7247-808-666; e-mail: crysdata@fiz-karlsruhe.de, http://www.fiz-karlsruhe.de/request_for_deposited_data.html) on quoting the deposition number CSD-427843.

Table 1. Crystal data and structure refinement of $PbSrGeO_4$ (space group: $P2_12_12_1$; standard deviations in parentheses where applicable).

Empirical formula	$PbSrGeO_4$
Molar mass, g mol^{-1}	431.40
Crystal system	orthorhombic
Space group	$P2_12_12_1$ (no. 19)
Lattice parameters from powder data	
Powder diffractometer	STOE Stadi P
Radiation	MoK_{α_1} ($\lambda = 70.93$ pm)
a, pm	994.08(8)
b, pm	730.84(7)
c, pm	598.88(6)
V, Å^3	435.09(9)
Single crystal data	
Single crystal diffractometer	Enraf-Nonius Kappa CCD
Radiation	MoK_α ($\lambda = 71.073$ pm) (graded multilayer X-ray optics)
Temperature, K	293(2)
a, pm	995.40(2)
b, pm	732.44(2)
c, pm	599.42(2)
V, Å^3	437.02(2)
Formula units per cell	4
Calculated density, g cm^{-3}	6.56
$F(000)$, e	736
Crystal size, mm^3	$0.01 \times 0.01 \times 0.02$
Absorption coefficient, mm^{-1}	57.3
Absorption correction	multi-scan (Scalepack [13])
θ range, deg	3.45–34.99
Range in *hkl*	$-9 \le h \le 9$, $-11 \le k \le 11$, $-16 \le l \le 15$
Total no. of reflections	1914
Independent reflections	1914
Reflections with $I > 2\,\sigma(I)/R_\sigma$	1895/0.0246
Data/ref. parameters	1914/66
Goodness-of-fit on F_i^2	1.078
Final indices R_1/wR_2 [$I > 2\,\sigma(I)$]	0.0380/0.0992
Final indices R_1/wR_2 (all data)	0.0385/0.0997
BASF	0.49(2)
Largest diff. peak and hole, e Å^{-3}	5.53/−3.94

Table 2. Atomic coordinates (Wyckoff positions 4*a* for all atoms) and equivalent isotropic displacement parameters U_{eq} (Å^2) of $PbSrGeO_4$ (space group: $P2_12_12_1$; standard deviations in parentheses). U_{eq} is defined as one third of the trace of the orthogonalized U_{ij} tensor.

Atom	x	y	z	U_{eq}
Pb1	0.65884(4)	0.31141(6)	0.18412(7)	0.0107(2)
Ge1	0.3372(2)	0.2876(2)	0.2737(2)	0.0055(2)
Sr1	0.04050(9)	0.5014(2)	0.2315(2)	0.0036(2)
O1	0.1807(9)	0.189(2)	0.205(2)	0.01(2)
O2	0.424(2)	0.1984(16)	0.5016(17)	0.017(2)
O3	0.300(2)	0.514(2)	0.355(2)	0.014(2)
O4	0.4428(8)	0.263(2)	0.039(2)	0.01(2)

Vibrational spectra

The Raman spectrum of a single crystal of $PbSrGeO_4$ was recorded with a Horiba Jobin Yvon LabRAM-HR 800 Raman micro-spectrometer in the spectral range of 100 – 4000 cm^{-1}. The sample was excited using the 532 nm emission line of a frequency-doubled 100 mW Nd:YAG laser and the 633 nm emission line of a 17 mW helium neon laser under an Olympus 100× objective lens. The diameter of the laser spot on the surface was approximately 1 μm. The scattered light was dispersed by an optical grating with 1800 lines mm^{-1} and collected by a 1024×256 open electrode CCD detector. The spectral resolution, determined by measuring the Rayleigh line, was less than 2 cm^{-1}. The spectrum was recorded unpolarized. The accuracy of the Raman line shifts, calibrated by regularly measuring the Rayleigh line, was in the order of 0.5 cm^{-1}. Second-order polynomial and convoluted Gaussian-Lorentzian functions were fitted to the background and Raman bands, respectively, using the built-in spectrometer software LabSpec.

DFT calculations

Electronic structure calculations were performed using the Vienna *ab initio* simulation package (Vasp) [17, 18] which is based on density functional theory (DFT) and plane wave basis sets. Projector-augmented waves (PAW) [19] were used, and contributions of correlation and exchange were treated in the generalized-gradient approximation (GGA) as described by Perdew, Burke and Ernzerhof [20]. The plane wave cutoff energy was 300 eV, and the total energy convergence criterion 10^{-5} eV. A three-dimensional grid of the charge density and the electron localization function (ELF) [21, 22] were calculated. In density functional theory, ELF depends on the excess of local kinetic energy due

Table 3. Anisotropic displacement parameters (U_{ij}/Å^2) for $PbSrGeO_4$ (space group: $P2_12_12_1$; standard deviations in parentheses).

Atom	U_{11}	U_{22}	U_{33}	U_{23}	U_{13}	U_{12}
Pb1	0.0087(2)	0.0101(2)	0.0134(2)	−0.0029(2)	−0.0025(2)	0.0008(2)
Ge1	0.0027(4)	0.0059(4)	0.0081(4)	0.0004(3)	−0.0004(3)	0.0001(3)
Sr1	0.0018(3)	0.0029(4)	0.0063(3)	0.0004(3)	0.0011(2)	0.0005(2)
O1	0.006(3)	0.011(3)	0.012(3)	0.000(3)	0.001(2)	−0.001(3)
O2	0.015(4)	0.021(5)	0.014(4)	0.004(4)	−0.009(3)	0.004(4)
O3	0.014(4)	0.005(3)	0.022(4)	−0.003(3)	0.004(3)	−0.007(3)
O4	0.002(3)	0.017(4)	0.011(3)	0.002(3)	0.003(2)	0.000(3)

Table 4. Synopsis of selected bond lengths (pm) of $PbSrGeO_4$ (space group: $P2_12_12_1$) calculated with the single-crystal lattice parameters (standard deviations in parentheses).

Pb1–O3	223.1(9)	Sr1–O2	245.9(9)	Ge1–O2	174.4(9)
Pb1–O1	234.3(9)	Sr1–O4	253.1(9)	Ge1–O4	176.4(8)
Pb1–O4	234.7(9)	Sr1–O2	261.9(12)	Ge1–O1	176.6(9)
	∅ = 230.7	Sr1–O1	262.3(9)	Ge1–O3	176.7(7)
		Sr1–O3	268.3(10)		∅ = 176.0
		Sr1–O1	268.5(9)		
		Sr1–O4	270.7(9)		
		Sr1–O3	276.6(11)		
			∅ = 263.4		

to the Pauli principle as compared to a bosonic system. High values of ELF appear in regions of space where the Pauli principle does not increase the local kinetic energy and thus pairing of electrons plays an important role. These regions can be assigned either to covalent bonds or to lone pairs.

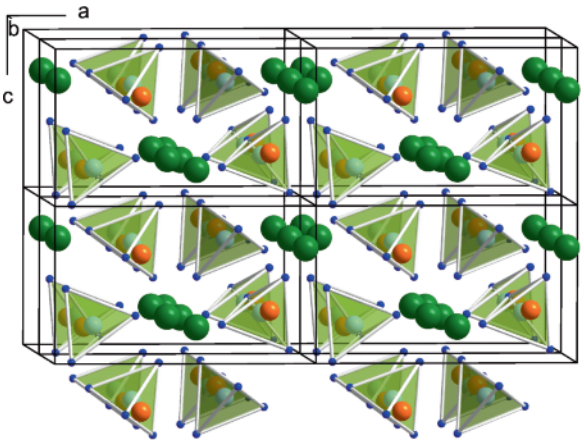

Fig. 2 (color online). Crystal structure of $PbSrGeO_4$ (space group: $P2_12_12_1$) showing a circular arrangement of $[GeO_4]^{4-}$ tetrahedra forming infinite tubes along $[0\bar{1}0]$ filled with Sr^{2+} ions (green). The Pb^{2+} ions (orange) are situated in the voids between the tetrahedra.

Results and Discussion

Crystal structure of $PbSrGeO_4$

The new lead strontium germanate crystallizes isotypically to the structure of $BaNdGaO_4$ in the orthorhombic space group $P2_12_12_1$ (no. 19) with four formula units per unit cell. The lead cation occupies the crystallographic position of the barium cation, whereas the strontium atom is situated on the position of the neodymium cation. The fundamental building unit is an isolated $[GeO_4]^{4-}$ tetrahedron. A repetition of a circular arrangement of six of these $[GeO_4]^{4-}$ tetrahedra leads to the formation of large channels along *b* that host the strontium ions which are eightfold coordinated by oxygen anions. Figs. 2 and 3 show the crystal structure of $PbSrGeO_4$ with a view along $[0\bar{1}0]$ and $[\bar{1}00]$, respectively. In addition to the three oxygen anions in the coordination sphere of the lead cation, a space for a lone pair can be distinguished, suggesting a pseudo-tetrahedral coordination of the lead cation. Because of that, special attention was given to the coordination sphere of the lead cation where the lone pair was visualized by the electron localization function (ELF) (isosurface value ELF = 0.97). The pseudo-tetrahedral coordination with lead-oxygen distances between 223.1(9) and 234.7(9) pm (mean value: 230.7 pm), and the lone pair is illustrated in the left hand part of Fig. 4. Obviously, this lone pair is stereochemically active as the position of the lead cation shifts towards the three oxygen atoms in comparison to the position of the barium cation in the isotypic compound $BaNdGaO_4$, whose coordination sphere is displayed in the right hand part of Fig. 4. A similar behavior can be found *e. g.* in the compound $PbVO_3$ that crystallizes in the perovskite structure possessing a lead cation with a stereochemically active lone pair [23]. In the case of $PbVO_3$, a slightly off-center shift of the Pb^{2+} cation out of the central position in the opposite direction to the lone pair can be recognized. The interatomic distances between the strontium cations and the oxygen anions are between 245.9(9) and 276.6(11) pm with a mean value

Table 5. Interatomic angles (deg) in $PbSrGeO_4$ (space group: $P2_12_12_1$), calculated with the single-crystal lattice parameters (standard deviations in parentheses).

O2–Ge1–O4	106.9(5)	O4–Ge1–O1	107.3(4)	O4–Ge1–O3	116.2(5)
O2–Ge1–O1	117.8(5)	O2–Ge1–O3	104.0(5)	O1–Ge1–O3	105.1(4)
					∅ = 109.6
O3–Pb1–O1	83.0(3)	O3–Pb1–O4	89.1(4)	O1–Pb1–O4	73.5(3)
					∅ = 81.9

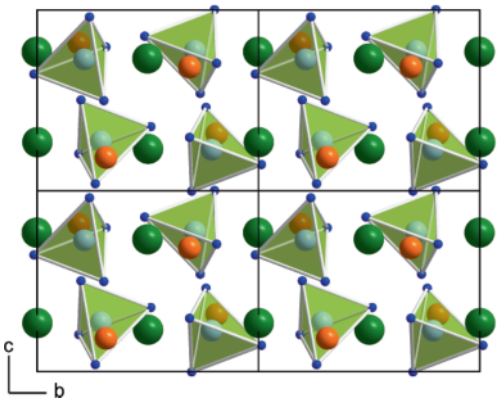

Fig. 3 (color online). Crystal structure of $PbSrGeO_4$ (space group: $P2_12_12_1$) with a view along [$\bar{1}$00].

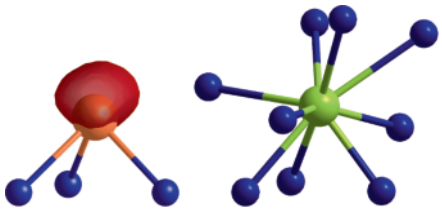

Fig. 4 (color online). Comparison of the coordination spheres of the Pb^{2+} ion with the lone pair visualized by the electron localization function (ELF) (isosurface value ELF = 0.97) and the Ba^{2+} cation (right) in the crystal structure of $BaNdGaO_4$ [1].

of 263.4 pm. Fig. 5 shows the coordination sphere of the strontium cations. The germanium-oxygen bond lengths in the tetrahedra vary from 174.4(9) to 176.7(9) pm with a mean value of 176.0 pm, and the O–Ge–O bond angles range from 104.0(5) to 117.8(5)° (average value: 109.5°). Both values are comparable with those of other compounds containing GeO_4 tetrahedra [6, 24, 25]. It should be noted that there exist further compounds that crystallize in the $BaNdGaO_4$ structure type, *e. g.* $BaLaGaO_4$ [1], α-$NaCuPO_4$ [26], $SrTlVO_4$ [27], $KSrVO_4$ [28], and $BaLaAlO_4$ [29].

The bond valence sums for all atoms in $PbSrGeO_4$ were calculated from the crystal structure using the bond-length/bond-strength concept ($\sum V$) [30, 31] and the CHARDI concept (*char*ge *di*stribution in solids, $\sum Q$) [32]. Table 6 shows the formal ionic charges received from the calculations which correspond well to the expected values.

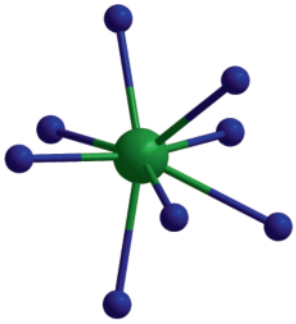

Fig. 5 (color online). Coordination sphere of the Sr^{2+} (green) cation in $PbSrGeO_4$.

Table 6. Charge distribution in $PbSrGeO_4$ (space group: $P2_12_12_1$), calculated with the bond-length/bond-strength ($\sum V$) and the CHARDI ($\sum Q$) concept.

	Pb1	Ge1	Sr1	O1	O2	O3	O4
$\sum V$	1.79	3.87	1.88	−1.95	−2.07	−1.79	−2.02
$\sum Q$	1.89	4.06	2.05	−2.06	−2.17	−1.67	−2.10

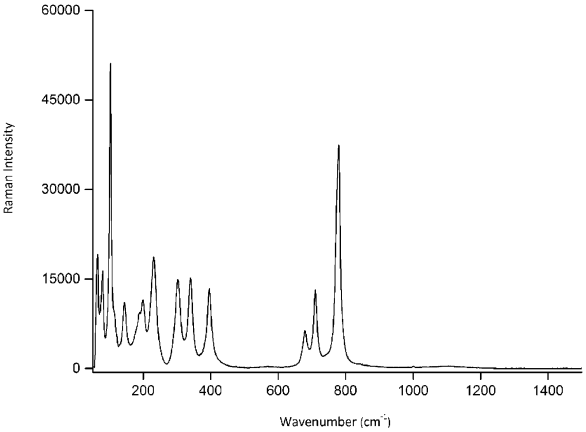

Fig. 6. Single-crystal Raman spectrum of $PbSrGeO_4$ in the range of 50 – 1500 cm^{-1}.

Furthermore, the MAPLE value (*MA*delung *P*art of *L*attice *E*nergy) was calculated from the crystal structure to compare it with the sum of the MAPLE values of the binary components PbO [33], SrO [34], and GeO_2 [35]. The difference between the values for the product and the sum of the educts amounts to 1.65 %.

Raman spectroscopy

The Raman spectroscopic measurements were performed on a single crystal of $PbSrGeO_4$. Fig. 6 shows

the Raman spectrum of $PbSrGeO_4$. The bands between 680 and 800 cm^{-1} can be interpreted as stretching vibrations [36, 37] of the GeO_4 tetrahedron, and bands in the range of 300 to 400 cm^{-1} can probably also be assigned to the bending modes of the GeO_4 tetrahedron [38]. Bands below 200 cm^{-1} may arise from mixed vibrations of the GeO_4 tetrahedron [36]. Presumably, these vibrations overlap with vibrations of the pseudo-tetrahedrally coordinated lead cation [38].

Conclusions

The novel lead strontium germanate $PbSrGeO_4$ marks a new compound in the group of germanates. It crystallizes in the space group $P2_12_12_1$ and is one of a few compounds that are isotypic to the structure of $BaNdGaO_4$. The main structural characteristics are isolated GeO_4 tetrahedra, eightfold-coordinated strontium cations, and pseudo-tetrahedrally coordinated lead cations exhibiting a stereoactive lone pair.

[1] I. Rüter, Hk. Müller-Buschbaum, *Z. Anorg. Allg. Chem.* **1990**, *584*, 119.
[2] J. H. Zhang, C. L. Hu, X. Xu, F. Kong, J. G. Mao, *Inorg. Chem.* **2011**, *50*, 1973.
[3] H. X. Zhang, J. Zhang, S. T. Zheng, G. M. Wang, G. Y. Yang, *Inorg. Chem.* **2004**, *43*, 6148.
[4] G. J. Cao, W. H. Fang, S. T. Zheng, G. Y. Yang, *Inorg. Chem. Commun.* **2010**, *13*, 1047.
[5] X. Xu, C. L. Hu, F. Kong, J. H. Zhang, J. G. Mao, *Inorg. Chem.* **2011**, *50*, 8861.
[6] J. H. Zhang, F. Kong, J. G. Mao, *Inorg. Chem.* **2011**, *50*, 3037.
[7] G. Heymann, H. Huppertz, *J. Solid State Chem.* **2006**, *179*, 370.
[8] M. I. Kay, R. E. Newnham, R. W. Wolfe, *Ferroelectrics* **1975**, *9*, 1.
[9] A. Ogg, *Philos. Mag. Ser.* **1928**, *5*, 354.
[10] J. A. McGinnety, *Acta Crystallogr.* **1972**, *B28*, 2845.
[11] Y. C. Hao, C. L. Hu, X. Xu, F. Kong, J. G. Mao, *Inorg. Chem.* **2013**, *52*, 13644.
[12] B. Petermüller, L. L. Petschnig, K. Wurst, G. Heymann, H. Huppertz, *Inorg. Chem.* **2014**, submitted.
[13] Z. Otwinowski, W. Minor in *Methods in Enzymology*, Vol. 276, *Macromolecular Crystallography*, Part A (Eds.: C. W. Carter Jr, R. M. Sweet), Academic Press, New York, **1997**, pp. 307.
[14] G. M. Sheldrick, SHELXS-13 and SHELXL-13, Program Suite for the Solution and Refinement of Crystal Structures, University of Göttingen, Göttingen (Germany) **2013**.
[15] G. M. Sheldrick, *Acta Crystallogr.* **2008**, *A64*, 112.
[16] K. Brandenburg, DIAMOND (version 3.2i), Crystal and Molecular Structure Visualization, Crystal Impact – H. Putz & K. Brandenburg GbR, Bonn (Germany) **2012**. See also: http://www.crystalimpact.com/diamond/.
[17] G. Kresse, J. Hafner, *Phys. Rev. B* **1994**, *49*, 14251.
[18] G. Kresse, J. Furthmüller, *Comput. Mater. Sci.* **1996**, *6*, 15.
[19] P. E. Blöchl, *Phys. Rev. B* **1994**, *50*, 17953.
[20] J. P. Perdew, K. Burke, M. Ernzerhof, *Phys. Rev. Lett.* **1996**, *77*, 3865.
[21] B. Silvi, A. Savin, *Nature* **1994**, *371*, 683.
[22] A. D. Becke, K. E. Edgecombe, *J. Chem. Phys.* **1990**, *92*, 5397.
[23] R. V. Shpanchenko, V. V. Chernaya, A. A. Tsirlin, P. S. Chizhov, D. E. Sklovsky, E. V. Antipov, E. P. Khlybov, V. Pomjakushin, A. M. Balagurov, J. E. Medvedeva, E. E. Kaul, C. Geibel, *Chem. Mater.* **2004**, *16*, 3267.
[24] P. Brandão, M. S. Reis, Z. Gai, A. M. dos Santos, *J. Solid State Chem.* **2013**, *198*, 39.
[25] M. A. Monge, E. Gutiérrez-Puebla, C. Cascales, J. A. Campá, *Chem. Mater.* **2000**, *12*, 1926.
[26] M. Quarton, A. W. Kolsi, *Acta Crystallogr.* **1983**, *C39*, 664.
[27] J. Boje, Hk. Müller-Buschbaum, *Z. Anorg. Allg. Chem.* **1992**, *611*, 137.
[28] M. Azrour, L. El Ammari, Y. Le Fur, B. Elouadi, *Mater. Res. Bull.* **2000**, *35*, 263.
[29] L. M. Kovba, L. N. Lykova, E. V. Antipov, *Koord. Khimiya* **1985**, *11*, 1574.
[30] I. D. Brown, D. Altermatt, *Acta Crystallogr.* **1985**, *B41*, 244.
[31] N. E. Brese, M. O'Keeffe, *Acta Crystallogr.* **1991**, *B47*, 192.
[32] R. Hoppe, S. Voigt, H. Glaum, J. Kissel, H. P. Müller, K. Bernet, *J. Less Common Met.* **1989**, *156*, 105.
[33] J. Leciejewicz, *Acta Crystallogr.* **1961**, *14*, 66.
[34] M. Zinkevich, *J. Solid State Chem.* **2005**, *178*, 2818.
[35] K. J. Seifert, H. Nowotny, E. Hauser, *Monatsh. Chem.* **1971**, *102*, 1006.
[36] V. D. Zhuravlev, A. P. Tyutyunnik, V. G. Zubkov, L. A. Perelyaeva, I. V. Baklanova, A. L. Blinova, *J. Solid State Chem.* **2012**, *194*, 32.
[37] F. Guyot, H. Boyer, M. Madon, B. Velde, J. P. Poirier, *Phys. Chem. Miner.* **1986**, *13*, 91.
[38] V. N. Sigaev, I. Gregora, P. Pernice, B. Champagnon, E. N. Smelyanskaya, A. Aronne, P. D. Sarkisov, *J. Non. Cryst. Solids* **2001**, *279*, 136.